

Lawrence Berkeley National Laboratory

Recent Work

Title

SOLUTION-SIDE TRANSPORT PROCESSES IN THE ELECTROPOLISH-ING OP COPPER IN PHOSPHORIC ACID

Permalink

<https://escholarship.org/uc/item/8qh4q9rs>

Authors

Kojima, K.
Tobias, C.W.

Publication Date

1972-07-01

Submitted to J. of the
Electrochemical Society

LAWRENCE
RADIATION LABORATORY

LBL-1106
Preprint c.1

LIBRARY AND
DOCUMENTS SECTION

SOLUTION-SIDE TRANSPORT PROCESSES IN THE
ELECTROPOLISHING OF COPPER IN PHOSPHORIC ACID

K. Kojima and C. W. Tobias

July 1972

Prepared for the U. S. Atomic Energy
Commission under Contract W-7405-ENG-48



For Reference

Not to be taken from this room

LBL-1106
c.1

DISCLAIMER

This document was prepared as an account of work sponsored by the United States Government. While this document is believed to contain correct information, neither the United States Government nor any agency thereof, nor the Regents of the University of California, nor any of their employees, makes any warranty, express or implied, or assumes any legal responsibility for the accuracy, completeness, or usefulness of any information, apparatus, product, or process disclosed, or represents that its use would not infringe privately owned rights. Reference herein to any specific commercial product, process, or service by its trade name, trademark, manufacturer, or otherwise, does not necessarily constitute or imply its endorsement, recommendation, or favoring by the United States Government or any agency thereof, or the Regents of the University of California. The views and opinions of authors expressed herein do not necessarily state or reflect those of the United States Government or any agency thereof or the Regents of the University of California.

SOLUTION-SIDE TRANSPORT PROCESSES IN THE ELECTROPOLISHING
OF COPPER IN PHOSPHORIC ACID

K. Kojima and C. W. Tobias

Inorganic Materials Research Division,
Lawrence Berkeley Laboratory, and
Department of Chemical Engineering;
University of California, Berkeley

July 1972

ABSTRACT

The unsteady state anodic dissolution of copper in 5 - 10 M phosphoric acid was carried out in the absence of convection, under galvanostatic and potentiostatic conditions. At a given bulk concentration of H_3PO_4 , the product of current density, i , and the square root of the time (t_s) of onset of sharp potential rise (or abrupt decline of current) is nearly constant in the active dissolution range. $i\sqrt{t_s}$ decreases with increasing acid concentration. The transition times found are in substantial agreement with those reported by Elmore and Edwards. By using the most reliable diffusivity data available for phosphoric acid and for anodically formed copper phosphate, it is shown that the rate limiting step in the active dissolution regime is the transport of copper phosphate from the electrode surface into the bulk solution. The peak current phenomena reported by numerous authors for steady state potentiostatic dissolution can be best interpreted by assuming rapid increase of coverage of the anode surface with solid reaction product after the critical solubility limit of copper phosphate is reached at the surface. The

Key Words: Electropolishing of copper Mass transport
Anodic dissolution of copper Phosphoric acid -role of-transport-
in electropolishing of copper

concentration of phosphoric acid at the surface up to and including the peak current density where the critical solubility of copper phosphate is exceeded, remains finite. The magnitude of the peak current density can be predicted by considering the transport of copper phosphate away from the surface to be the limiting transport process.

INTRODUCTION

Electropolishing of copper in concentrated phosphoric acid occurs under diffusion control (1,2). Although the constancy of the product of current density and square root of transition time in galvanostatic unsteady state dissolution has been confirmed (3,4,5,6), identification of the rate-determining species at the current plateau (2,3,4,7,8) has remained a controversial problem. Edwards (3) and Wagner (9) proposed that transport of one of the reactants from the bulk electrolyte to the anode surface is the rate-limiting process. The role of diffusion of water on the limiting current was discussed by Petit (8). On the other hand, Elmore (4,10) claimed that without significant increase of applied cell voltage the current begins to decrease when the concentration of the dissolved copper species at the anode surface reaches the solubility limit. Hickling and Higgins (7) found that the limiting current decreases proportionally to the decrease of concentration difference of cupric ions between the anode surface and the bulk electrolyte. However, Hickling and Higgins' test was performed in dilute phosphoric acid (2M/1), where electropolishing is not possible.

In the decades that have passed since the two essentially opposite transport mechanisms have been proposed by Elmore and Edwards, a great deal of information has been developed on properties of the phosphoric acid-copper phosphate-water system. It appears therefore timely and worthwhile to undertake a re-examination of the question of the transport mechanism responsible for the smoothing and brightening

action during electropolishing. Optical observations (11) of the copper surface undergoing dissolution, surface impedance measurements (12) and ellipsometric studies (13), wetting characteristics (Mercury test) (1) all point to the fact that visible as well as invisible surface layers play an important role in the polishing process. In a qualitative study, preliminary to the present investigation, the present authors have found that in the unsteady state active dissolution of copper in phosphoric acid the surface is free of solids. In steady state electropolishing, however, solid material exists on and near the surface. These findings corroborate the observations reported earlier among others by Lorking(11), and Hoar et al. (1).

In the following unsteady state dissolution experiments are described, which were conducted deliberately under conditions similar to those by Elmore and Edwards. Transition times in the active dissolution regime are interpreted using the best available transport property values.

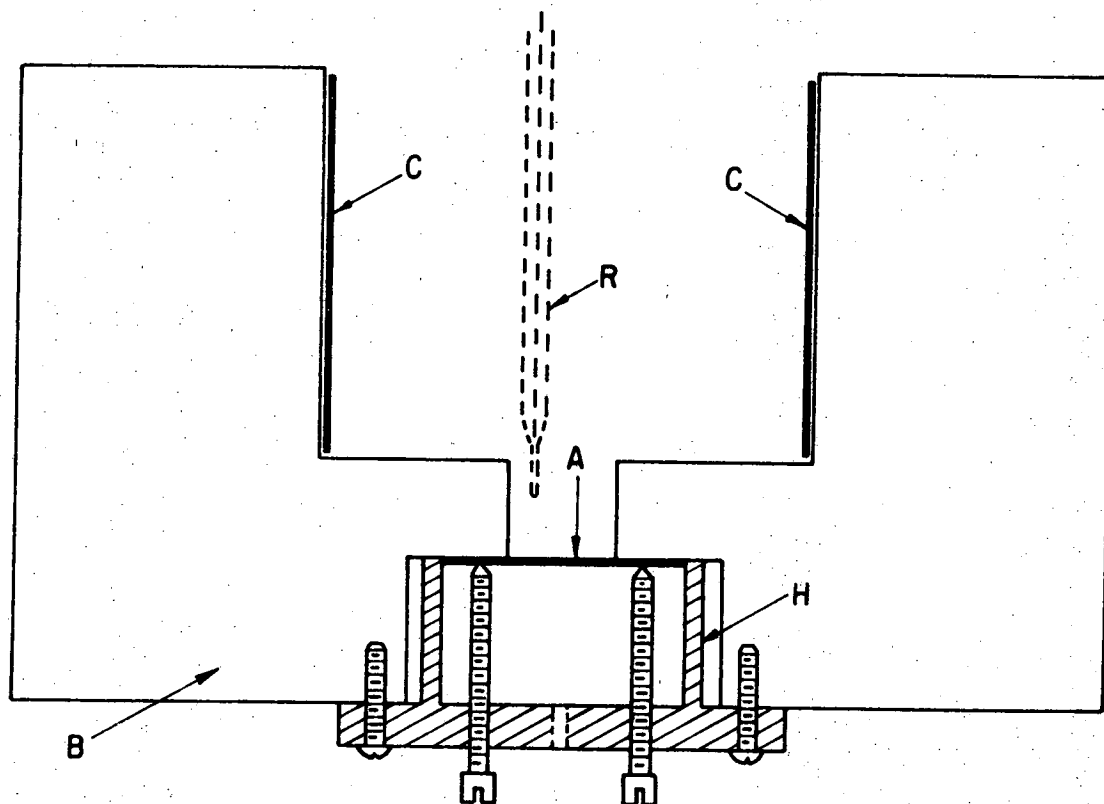
The transport mechanism proposed on the basis of these unsteady state experiments is then subjected to critical test using the peak current density data obtained by Hoar and Rockwell under steady state potentiostatic conditions.

DISSOLUTION OF COPPER UNDER GALVANOSTATIC CONDITIONS

Experimental Apparatus and Procedure

The experimental cell is shown schematically in Fig. 1. This simple cell was purposely designed to resemble the cell geometry employed by both Elmore (4,10) and Edwards (3). The straight wall of the cylindrical anode compartment parallel to the direction of electric current flow and the ratio of the height of the anode compartment to its diameter provide a geometry that gives a reasonably uniform current density distribution over the entire surface of the portion of the anode exposed to the electrolyte. The apparent area of the portion of the anode exposed to the electrolyte is 1.46 cm^2 and the inside area of the cylindrical cathode exposed to the electrolyte is 38 cm^2 . During cell operation, the anode disk was in a horizontal position, facing upward. Since a more dense solution is forming upon anodic dissolution of copper, this configuration assures absence of convection during experimental runs. The laminar free convection occurring at the vertical cathode didn't disturb the immobile solution in the anode compartment within the relatively short time spans (0.2 - 100 sec) involved in these experiments.

Analytical grade phosphoric acid (Baker, 85.9%) was diluted to desired concentrations (5 or 10 M) for each experiment. The cathode was made from 99.9% polycrystalline copper; the anodes were prepared either from the same material, or cut from single crystals parallel to the (111) plane. Anode specimens were mechanically polished, washed with water and acetone, and subsequently anodically etched in concentrated



XBL 7111-7538

Fig. 1. Side view of the experimental cell.
A: Anode disk 1.27 cm dia exposed B: Plexiglass cell body
C: 5 cm dia copper cathode ring.
Anode compartment: 1.2 cm high, cathode compartment: 2.4 cm.
H: Plexiglass anode holder R: 0.06 cm O.d. reference capillary
junction. The reference electrode is a copper wire set in the
capillary tube.

H_3PO_4 . In a few instances chemical polish was used in a $HNO_3:H_3PO_4:HAc = 2:1:1$ vol. solution. Dissolution experiments were carried out at $22 \pm 1^\circ C$.

After the current was cut off, anodes were immediately removed, washed with water and acetone and dried at room temperature for weight loss measurements, or for microscopic observation of the surface. Anode surfaces were also observed in situ during dissolution under relatively low (10-45x) magnification. Constant current experiments were carried out by using external control of current (a) or, by potentiostatic control of the anode potential (b), involving approximately 2 - 7 ohm resistance between reference capillary tip, and anode surface.

a). Constant current supply was provided by an Electronic Measurements Model C 621 power supply. The cell voltage was recorded by Sargent Model MR recorder. This techniques was used for transition times of over 25 seconds. This range allowed observation of the surface in situ under low level (10-45x) magnification.

b). Anotrol Model 4100 Potentiostat was employed to provide a constant potential between a reference electrode and the anode surface. In the active dissolution region the resistance between capillary tip and surface was sufficiently large compared to the impedance associated with the electrode reaction, so that potential control in this case corresponded to controlling current, at least up to the transition time. The current vs. time behavior was obtained by passing the cell current through a calibrated resistor and recording the resulting

potential drop on a Tektronix Model 531 oscilloscope. Transition times in the range of 0.2 - 5 seconds could be obtained with good reproducibility.

Visual Observation of the Anode Surface during Dissolution

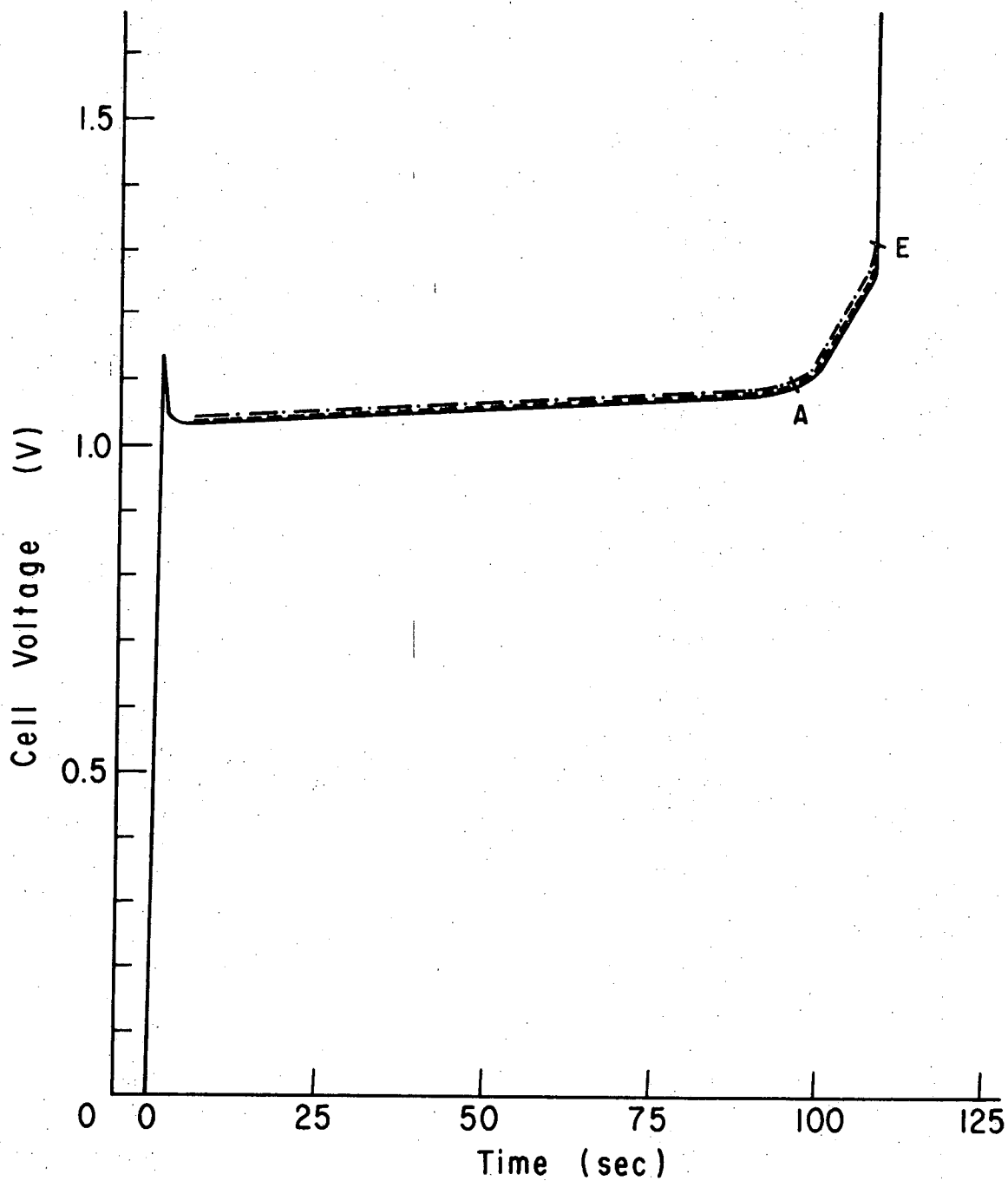
Typical cell voltage vs. time behavior in externally controlled constant current runs is illustrated in Fig. 2. After closing the circuit the cell voltage abruptly rises to a plateau and then increases only slightly (40-60mV) to point A, after which the increase is quite sharp (the first voltage jump). Visual observation under 10-45x magnification reveals, that at point A blue solid particles (probably copper phosphate) begins to form at the anode. As point E is reached (the second voltage jump) the number of particles becomes quite large; the blue color is spread over the entire surface. The onset of formation of small particles of blue color at point A becomes less distinct at higher applied current densities (above 0.05 A/cm^2). At the highest current density employed in these experiments, at $i = 0.0676 \text{ A/cm}^2$, identification of two separate potential breaks was no longer possible.

Valence of dissolution

Weight loss measurements were carried out in runs extended up to the transition point A. The apparent valence of dissolution n' was obtained from

$$n' = \frac{M \cdot I \cdot t}{F \cdot \Delta W}$$

where I:total current (A), t:time (sec), M:molecular weight of copper (g/gmole) F:Faraday, ΔW : weight loss (g). From eight measurements, up



XBL 7111-7540

Fig. 2. Cell voltage change with time for polycrystalline copper in 10.05M/l H₃PO₄, $i = 0.0362 \text{ A/cm}^2$ (six repeated runs are indicated by solid—, and dashed -- lines). The apparent valence is 2.0₃.

to $i = 0.038 \text{ A/cm}^2$ $n' = 2.0$ was obtained. In the following we shall assume that in the active dissolution regime, copper anodically dissolves in phosphoric acid with a valence of 2. Visual identification of the appearance of solid blue particles at the time when the voltage begins to rise rapidly in galvanostatic experiments suggests that the latter event is caused by the formation of solid copper phosphate at the anode surface. The change of concentration of reactants, or of reaction products at the anode surface is obtained by solving the diffusion equation:

$$\frac{\partial C}{\partial t} = D \frac{\partial^2 C}{\partial x^2}$$

with initial condition: $C = C(0)$ at $t = 0$

and boundary conditions: $C = C(0)$ at $x = \infty$

$$i = -nFD \left(\frac{\partial C}{\partial x} \right)_{x=0}$$

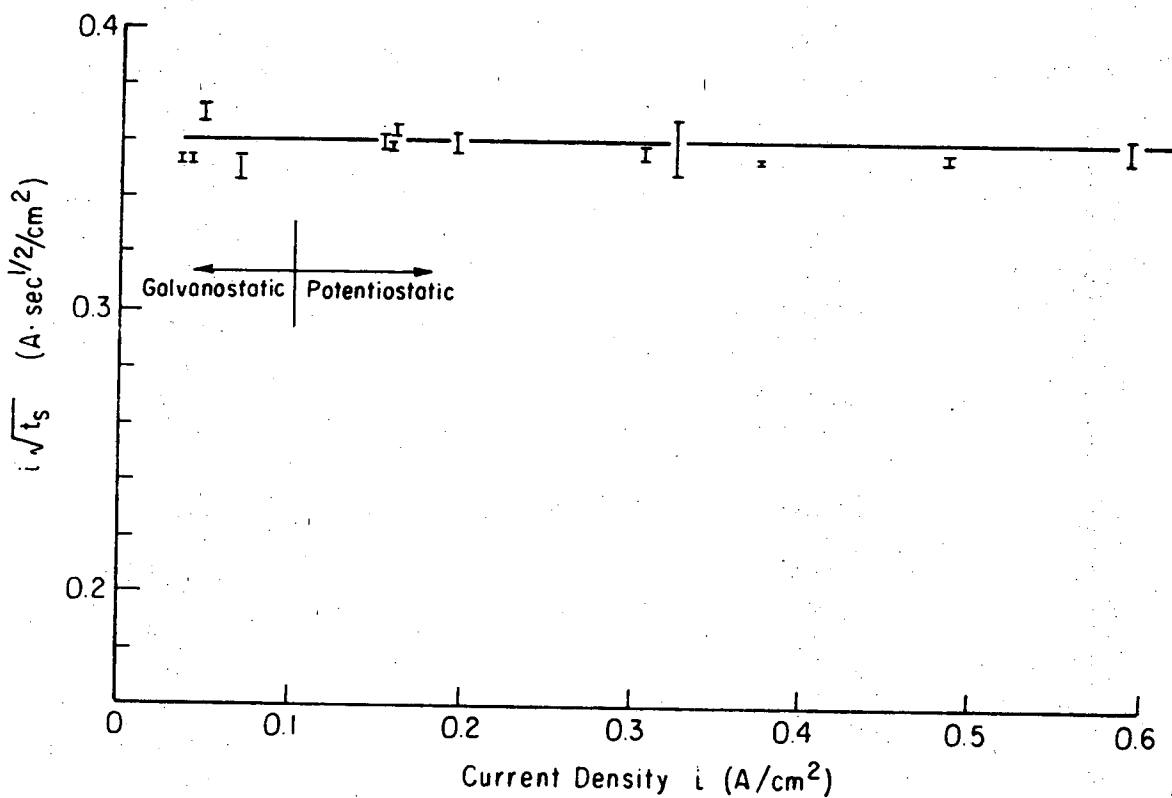
Neglecting migration effects, we get (Ref. 14)

$$|C(t) - C(0)|_{x=0} = \frac{2i}{nF} \left(\frac{t}{\pi D} \right)^{1/2} \quad (1)$$

where $C(0)$ and $C(t)$ are the concentration of a reactant, or of a product at the surface, respectively, and n is the number of electrons transferred in the electrode process per gmole (or gion) of the participating species considered.

The concentration of a reactant or a reaction product at the anode surface at the transition time $t = t_s$ has some characteristic value, solely determined by the bulk composition, and temperature, independent of applied constant current density.

Figure 3 includes results from about 90 individual experiments obtained by current control ($0.031 - 0.0676 \text{ A/cm}^2$) and potential control ($0.16 - 0.6 \text{ A/cm}^2$) in $10.0 \text{ M } \text{H}_3\text{PO}_4$. In this range of current densities, $i\sqrt{t_s} = 0.36 \pm 0.015$. Similar experiments conducted in $5 \text{ M } \text{H}_3\text{PO}_4$ yielded $i\sqrt{t_s} = 0.73 \pm 0.04$, again indicating, that the transition time t_s as defined by the time of onset of the first voltage jump, is controlled by transport of one of the reactants, or products.



XBL 727-6595

Fig. 3. Relation between $i\sqrt{t_s}$ and i in 10.05M H_3PO_4 . (111) face of single crystal (99.999%) was employed in runs at $i = 0.308, 0.485, \text{ and } 0.591 \text{ A/cm}^2$. All others involved were 99.9% polycrystalline copper. Number of experiments at a given current density: 3-10.

DISCUSSION

Comparison of Present Work with Previous Results

Figure 3 shows that $i\sqrt{t}_s$ is nearly independent of current density in the range of 0.03-0.6 A/cm². This is in good agreement with the results obtained by Elmore (4), Edwards (3), Krichmar (5) and Vozdvishensky, et.al. (6). In 10 M H₃PO₄ the values of $i\sqrt{t}_s$ obtained by interpolation from Elmore's and Edward's work are 0.36₈ (at 23.5 - 24°C) and 0.37₄ (at 25°C) respectively, very close to the value of 0.36 obtained in this research.

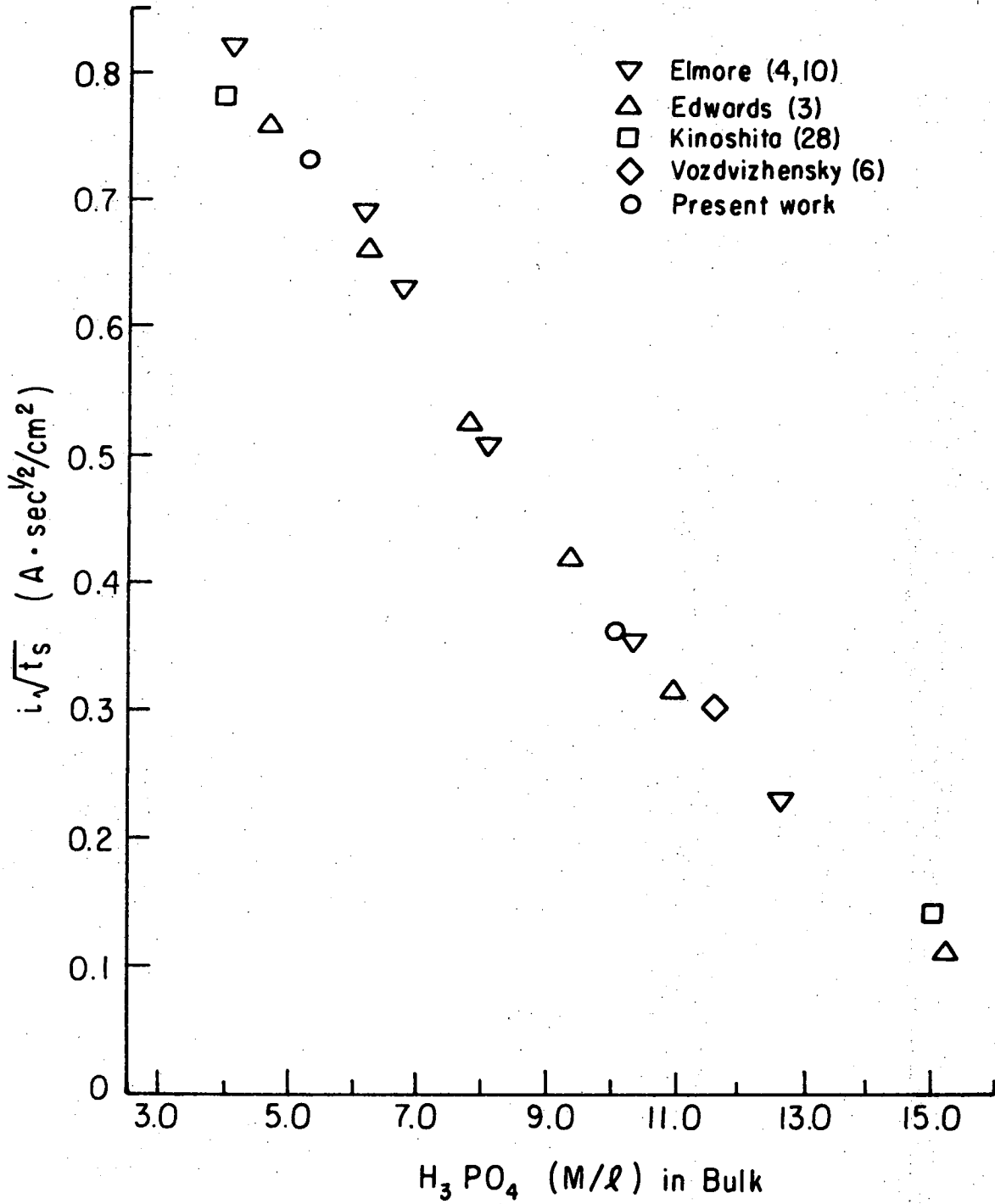
The apparent valence of dissolved copper obtained in this work, 2.0 for the active dissolution of copper, is in good agreement with the value 2.00 reported by Petit and Schmitt (15).

Relation between $i\sqrt{t}_s$ and the Concentration of Phosphoric Acid:

If the values of $i\sqrt{t}_s$ are characteristic of the properties of the electrolyte, it follows that they should be unique functions of the concentration of aqueous phosphoric acid at a given temperature. In Fig. 4 $i\sqrt{t}_s$ is plotted against the concentration of phosphoric acid. The values obtained by Elmore, Edwards, and by the present authors, are in good agreement with one another; $i\sqrt{t}_s$ decreases with increasing acid concentration. It is to be noted that the significance of this pattern of behavior was not recognized by the authors mentioned above.

Diffusion Kinetics

The reactants and reaction products in the active dissolution of copper move to or away from the anode by migration and diffusion. The

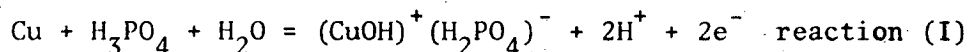


XBL 7111-7545

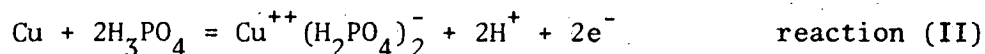
Fig. 4. Effect of the concentration of phosphoric acid in bulk, C_{rb} , on $i\sqrt{t_s}$.

diffusion layer is built up corresponding to the applied current density, time, diffusivity and transference number of a species participating in the process.

According to Laforge-Kantzer (16), copper dissolves in concentrated phosphoric acid along the following over-all reaction scheme



Krichmar and Galushko (17), on the other hand, claim that the copper dissolution reaction may be described by



The first cell voltage jump may be expected to result

- a) from the strong depletion of one of the reactants, that is, H_3PO_4 or H_2O in reaction I and H_3PO_4 in reaction II, and
- b) from the solubility limit of one of the reaction products (copper phosphate*) being exceeded and a high resistive film being formed on the anode.

In case a., the concentration of a reactant C_r at the anode surface decreases with time and reaches $C_r \rightarrow 0$ at $t = t_s$, causing a sharp increase of the concentration overpotential. Here, at $t = t_s$, the concentration of the reaction product is assumed to be below its solubility limit.

In case b., the concentration of the reactant at the anode surface

* We use the terminology "copper phosphate" to denote the dissolution product of copper in phosphoric acid.

doesn't reach $C_r \rightarrow 0$ at $t = t_s$.

Assuming that copper dissolution occurs with 100% current efficiency, the following relations (for derivation, see Appendix and also Ref. 18) are applicable at the anode surface in reaction I:

$$i = \frac{2F}{1 - t_{\text{CuOH}^+}} D_p \left| \nabla C_p \right| \quad \text{for copper phosphate} \quad (3)$$

$$i = \frac{F}{t_{\text{H}^+} - \frac{t_{\text{CuOH}^+}}{2}} D_r \left| \nabla C_r \right| \quad \text{for phosphoric acid} \quad (4)$$

In reaction II

$$i = \frac{2F}{1 - t_{\text{Cu}^{++}}} D_p \left| \nabla C_p \right| \quad \text{for copper phosphate} \quad (5)$$

and

$$i = \frac{F}{t_{\text{H}^+}} D_r \left| \nabla C_r \right| \quad \text{for phosphoric acid} \quad (6)$$

i , $t_{\text{Cu}^{++}}$, t_{H^+} , ∇ , D_p , and D_r are applied current-density, transference number of Cu^{++} , that of H^+ , gradient, diffusivity of copper phosphate, and that of phosphoric acid, respectively. Calculations of limiting current density in terms of water or H^+ concentration are not convenient because the necessary experimental data are not available. The diffusivity of phosphoric acid in the $\text{H}_3\text{PO}_4 - \text{H}_2\text{O}$ system has been measured at

25°C by O. W. Edwards and Huffman (19) and that of the anodic dissolution product of copper in phosphoric acid at 20°C by Krichmar, et al. (20).

We now choose phosphoric acid as the reactant and copper phosphate as the reaction product in our diffusion calculations.

(Case a.) If the first cell voltage jump is caused by the strong depletion of phosphoric acid at the anode surface, because of $C_r(t_s) = 0$ we get

$$i \left(\frac{t_s}{D_r} \right)^{1/2} = \frac{F}{2} \cdot \frac{\sqrt{\pi}}{t_{H^+} - \frac{1-t_{CuOH^+}}{2}} \cdot C_{rb} \quad \text{for reaction I} \quad (7)$$

and

$$i \left(\frac{t_s}{D_r} \right)^{1/2} = \frac{F}{2} \cdot \frac{\sqrt{\pi}}{t_{H^+}} \cdot C_{rb} \quad \text{for reaction II} \quad (8)$$

Assuming that the transference number of H^+ or $CuOH^+$ is constant, the term $i\sqrt{t_s/D_r}$ should be proportional to C_{rb} , the concentration of phosphoric acid in the bulk of the electrolyte, the driving force for the diffusion of phosphoric acid. The relation between $i\sqrt{t_s/D_r}$ and the concentration of phosphoric acid is shown by the solid curve in Fig. 5, where the values of $i\sqrt{t_s}$ measured by Elmore, Edwards, as well as those by the present authors are plotted. As shown, $i\sqrt{t_s/D_r}$ decreases sharply as the bulk concentration of phosphoric acid increases. A sharper decline of $i\sqrt{t_s/D_r}$ with bulk H_3PO_4 concentration would be obtained, if we were to use some average value of diffusivity between bulk and interface (D'_{rm}). This would correct upward the effective

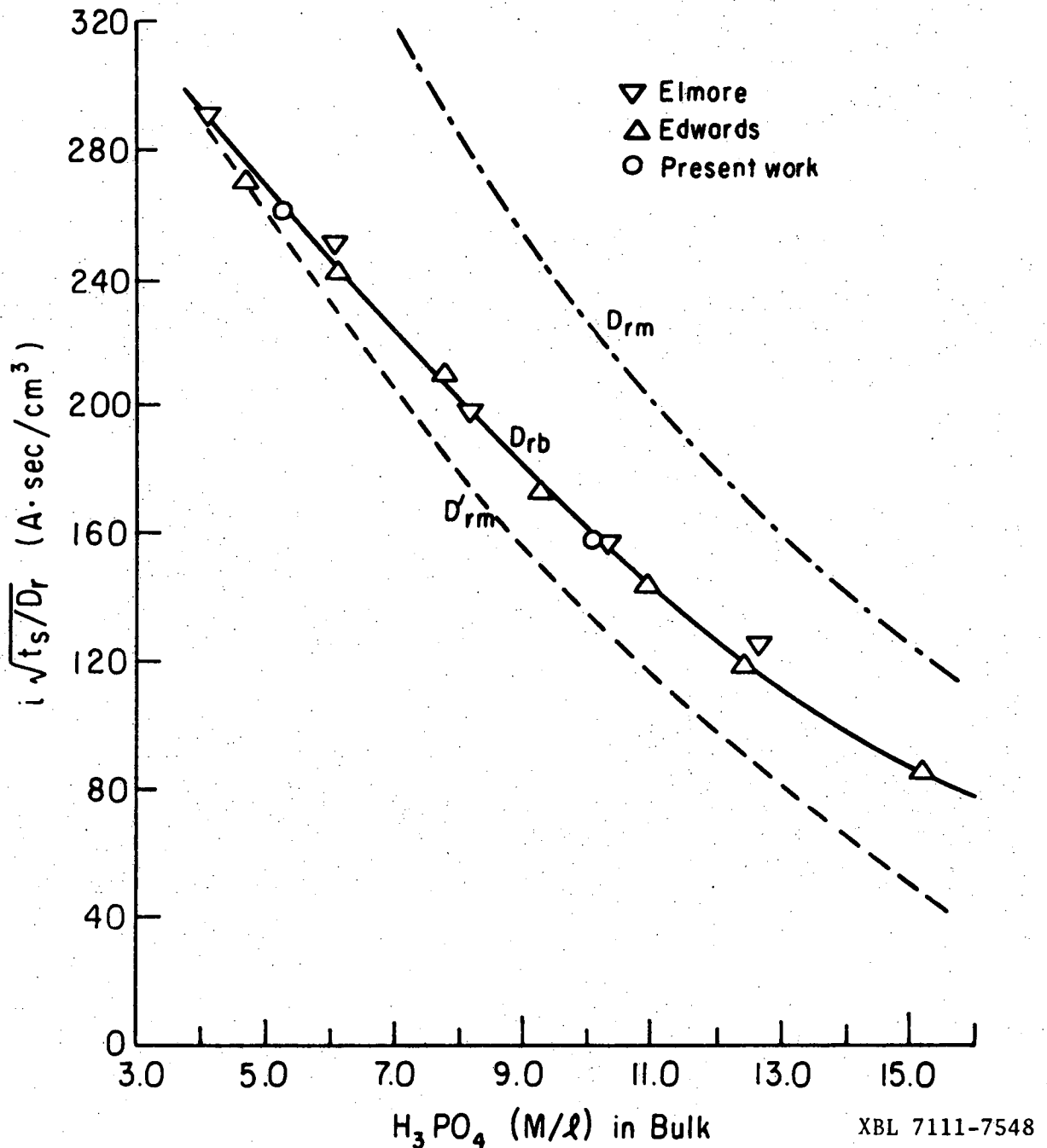


Fig. 5. Relation between $i\sqrt{t_s/D_r}$ and the concentration of phosphoric acid, C_{rb} . $i\sqrt{t_s/D_r}$ was obtained from Elmore, Edwards, and in the present work. ---curve indicates approximate pattern of experimental results of arithmetic mean diffusivity $D_{rm}^i = \frac{1}{2} (D_{rb} + D_{ro})$. D_{ro} : D_r for $(H_3PO_4) \rightarrow 0$. -.-.- curve indicates qualitative behavior for $D_{rm} = \frac{1}{2} (D_{rb} + D_{rs})$, where D_{rs} denotes the value of D_r at the critical solubility of copper phosphate. Because copper phosphate increases considerably the viscosity of electrolyte, $D_{rb} \gg D_{rs}$ is assumed.

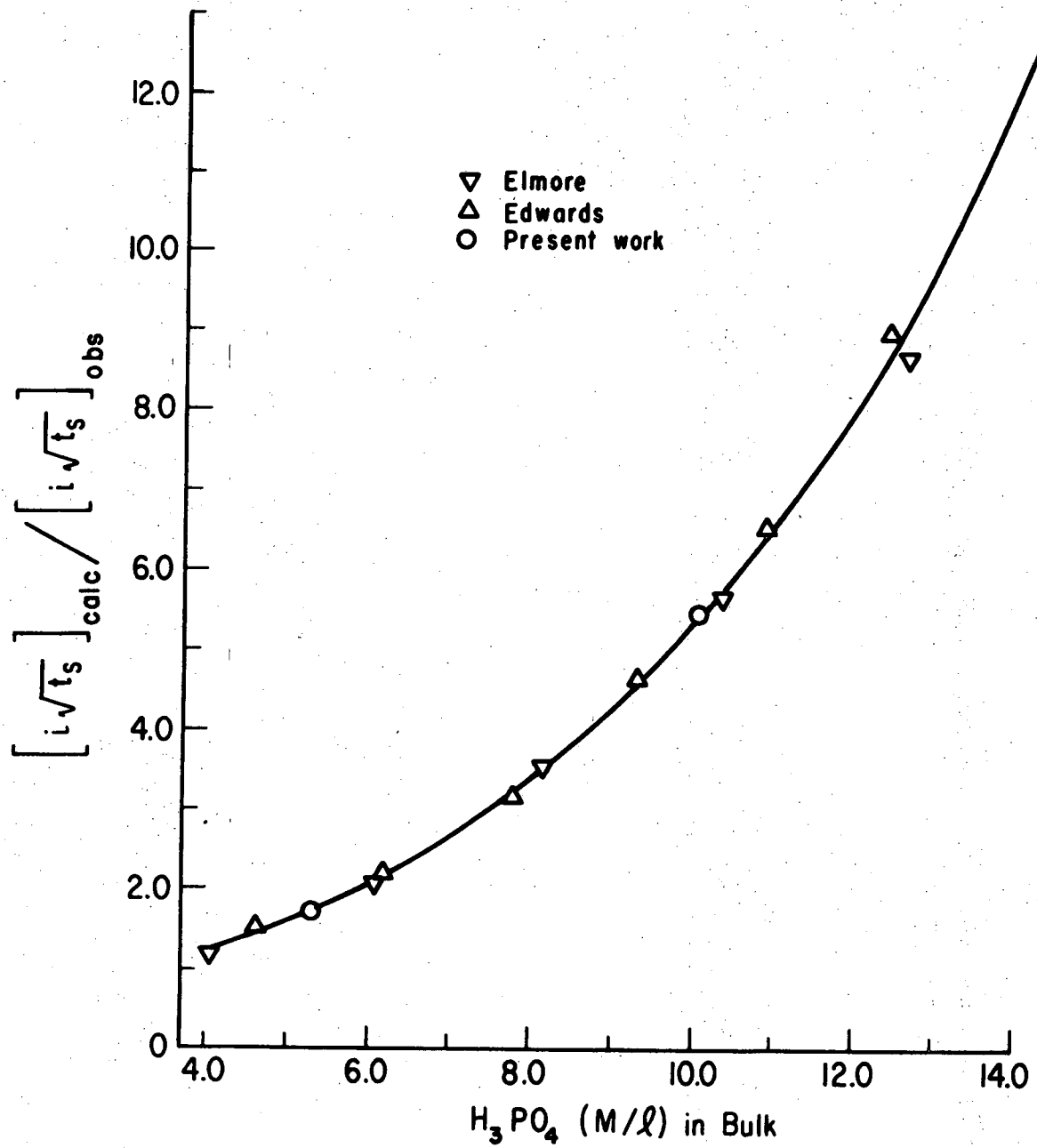
diffusivities. The correction would be proportionally larger, the higher bulk concentration, because $D'_{rm} = (1/2)(D_{rb} + D_{ro})$ and the diffusivity of H_3PO_4 at the interface, D_{ro} , has the same (highest) value irrespective of C_{rb} .

Qualitatively the reverse situation arises if we take into consideration the effect of copper phosphate at the anode surface on the diffusivity of phosphoric acid (case of D_{rm}): because of the presence of copper phosphate the viscosity is higher at the interface than in the bulk. Consequently the relationship between $i\sqrt{t_s/D_{rm}}$ * and H_3PO_4 concentration would be described by a curve lying above the one obtained by assuming $D_r = D_{rb}$. As a further test of the hypothesis involving phosphoric acid as the limiting reactant, the ratio of calculated vs. experimentally obtained $i\sqrt{t_s}$ values are plotted in Figure 6. For reaction II the calculated values were obtained by:

$$i(t_s)^{1/2}_{calc} = \frac{F}{2} (\pi D_r)^{1/2} C_{rb} \quad (9)$$

For diffusivities of phosphoric acid, the bulk values, D_{rb} , were employed, and the transference number of hydrogen ion, t_{H^+} , was assumed to be unity. It should be noted that both the use of arithmetic mean values of diffusivities between bulk and surface, as well as the assumption of lower transference number for the hydrogen ion causes the ratios plotted in Fig. 6 to increase, i.e., to depart further from correspondence of calculated vs. experimental values. Similarly, the discrepancy becomes larger, if we assume that the reaction stoichiometry is

* $D_{rm} = (1/2)(D_{rb} + D_{rs})$



XBL 7111-7550

Fig. 6. Relation between $i\sqrt{t_s}_{calc}/i\sqrt{t_s}_{obs}$ and the concentration of H_3PO_4 for strong depletion of H_3PO_4 at the anode surface (reaction II). $i\sqrt{t_s}_{calc}$ was obtained by Eq. (8) with D_{rb} .

(Case b.) We will now proceed and assume that the interfacial concentration of H_3PO_4 is not approaching zero at the anode surface, rather it will have some finite value. The transference number of hydrogen ions, t_{H^+} , then, will be close to unity, * and that of copper ions, $t_{Cu^{++}}$, will approach zero. For $C_p(0) = 0$ and $C_p(t_s) = C_{ps}$ we get

$$i \left(\frac{t_s}{D_p} \right)^{1/2} = \frac{F(\pi)^{1/2}}{1 - t_{CuOH^+}} C_{ps} \quad \text{reaction I} \quad (10)$$

or

$$i \left(\frac{t_s}{D_p} \right)^{1/2} = \frac{F(\pi)^{1/2}}{1 - t_{Cu^{++}}} C_{ps} \quad \text{reaction II} \quad (11)$$

Assuming $t_{CuOH^+} \rightarrow 0$ and $t_{Cu^{++}} \rightarrow 0$, we obtain the simplified relation:

$$i \left(\frac{t_s}{D_p} \right)^{1/2} = F(\pi)^{1/2} C_{ps} \quad (12)$$

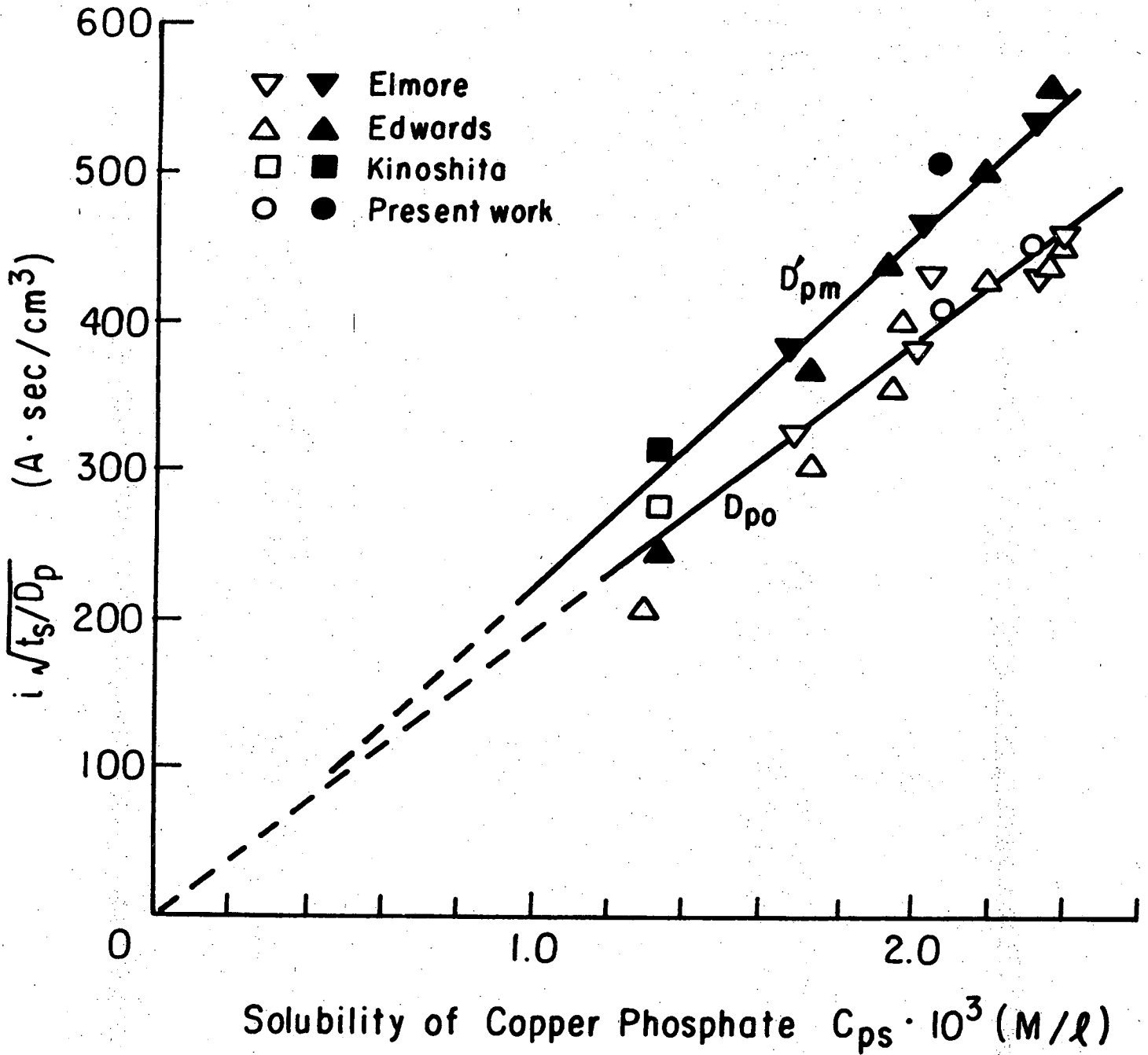
for both reactions I and II. If the first cell voltage jump is caused by reaching the solubility limit of copper phosphate, followed by the formation of a resistive film, $i\sqrt{t_s/D_p}$ should be proportional to the solubility of copper phosphate, C_{ps} . For purposes of this calculation we employ Hickling and Higgins' experimental values (7) for the solubility of Cu^{++} in phosphoric acid at 20°C. Diffusivities of anodically formed copper phosphate were measured by Krichmar, et al. (20). Because of the complex way in which the concentration dependent

* According to Kerker and Espenscheid (21) t_{H^+} in 4M H_3PO_4 is 0.89. In Chapman's critical review of transport properties (22) the range of $t_{H^+} = 0.93 \rightarrow 1.0$ is given for 4 \rightarrow 12 M H_3PO_4 .

diffusivity influences t_s , values of $i\sqrt{t_s/D_p}$ in figure 7 have been evaluated using two different diffusivities: 1) D_{po} , the diffusivity of Cu^{++} at very low concentration (i.e., corresponding to conditions in the bulk), and, 2) D'_{pm} , the arithmetic mean of D_{po} and D_{ps} (diffusivity at critical solubility). As shown in Fig. 7, in the range of phosphoric acid concentration (4-15 M) the value of $i\sqrt{t_s/D_{po}}$ or $i\sqrt{t_s/D'_{pm}}$, in fact, increases approximately directly proportionally with the solubility of copper phosphate (1.3 - 2.4 M/l).

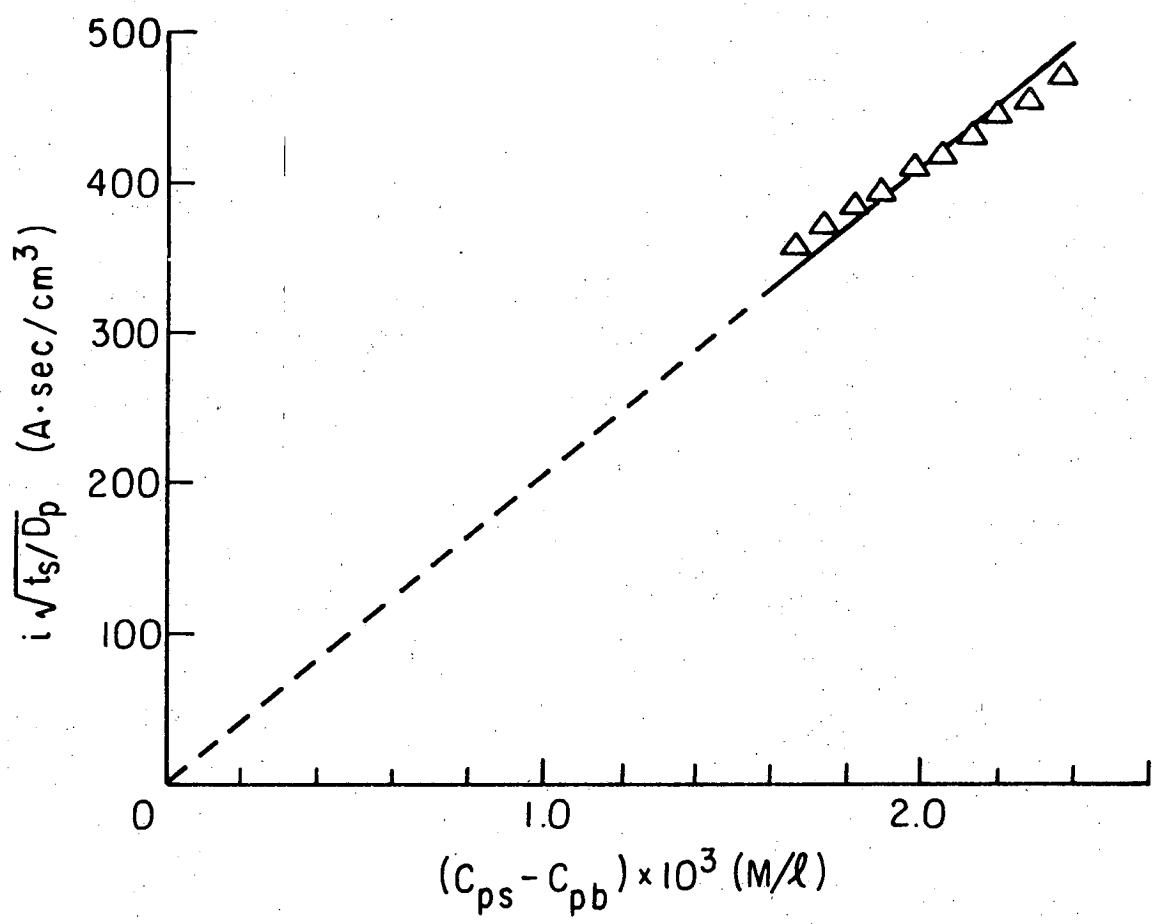
Another test can be made by examining the relation between $i\sqrt{t_s/D_p}$ and $(C_{ps} - C_{pb})$ for a fixed C_{ps} and a variable C_{pb} . Edwards (3) found that for a given phosphoric acid concentration the value of $i\sqrt{t_s}$ decreases with the increase of C_{pb} . However, because of lack of diffusivity data of copper phosphate the relation between $i\sqrt{t_s/D_p}$ and $(C_{ps} - C_{pb})$ was not investigated. This relation as evaluated by the present authors is shown in Fig. 8. $i\sqrt{t_s}$ and C_{pb} were obtained from Edwards (3). For the diffusivity of copper phosphate its value in the bulk phosphoric acid (50%) is used. Direct proportionality of $i\sqrt{t_s/D_p}$ to $(C_{ps} - C_{pb})$ is again demonstrated. Thus, in contrast to the interpretation of Edwards, his data on the effect of presence of Cu^{++} in the bulk electrolyte indicates that the onset of voltage rise is caused not by the depletion of H_3PO_4 , but rather by the accumulation of copper phosphate at the anode surface.

It remains to be tested whether the proportionality constant is in good agreement with the constant theoretically obtained. For the purpose of this test, the experimental values of $i\sqrt{t_s}$ are plotted



XBL 7111-7551

Fig. 7. Relation between $i\sqrt{t_s D_p}$ and the critical solubility of copper phosphate.
 $D_{po} : D_p$ at $C_p \rightarrow 0$ $D'_{pm} : (1/2)(D_{po} + D_{ps})$.



XBL727-6596

Fig. 8. Relation between $i\sqrt{t_s/D_p}$ and the concentration difference of copper phosphate between anode surface and bulk electrolyte. $i\sqrt{t_s}$ and C_{pb} data were taken from Edwards (3).

against

$$i(t_s)_{\text{calc}}^{1/2} = F(\pi D_p)^{1/2} C_{ps} \quad (12')$$

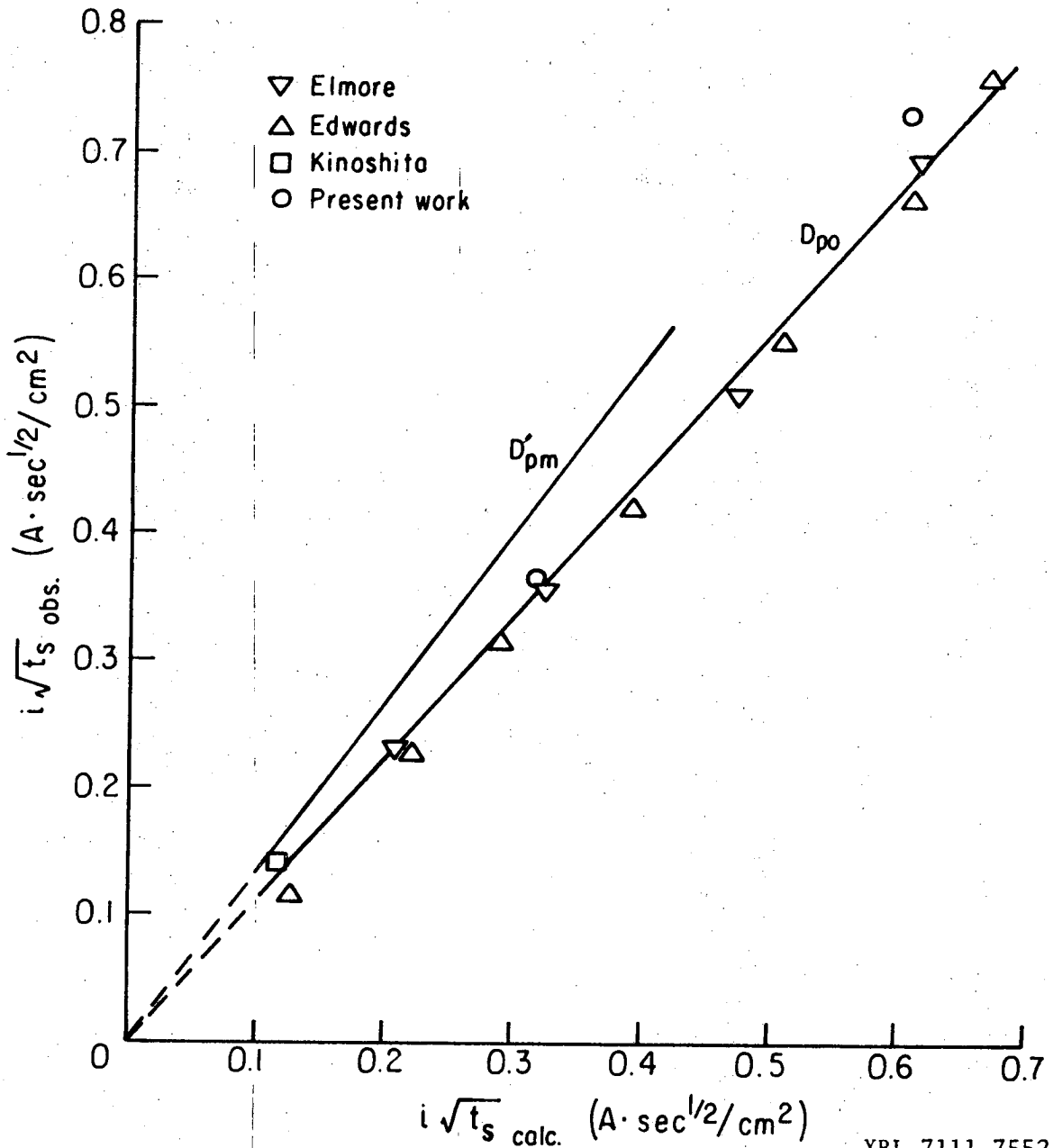
Figure 9 shows that for D_{po} the calculated values are over a wide range in reasonable agreement with the measured values of $i(t_s)^{1/2}$. The ratios of calculated to measured values are about 1.1 for D_{po} and 1.3 for D'_{pm} respectively.* The above argument gives strong support to the view that the first cell voltage jump is caused by reaching the solubility limit of copper phosphate followed by the formation of a resistive film (18, 23). If the first cell voltage jump is really caused by the critical solubility of copper phosphate, the concentration of phosphoric acid at the anode surface at $t = t_s$, C_{rs} , is higher than zero. In Fig. 10, values of C_{rs} , calculated by using Eq. 7 or 8 are compared to those obtained by chemical analysis** (17,24). The calculated C_{rs} values are in fairly good agreement with the measured concentrations of free phosphoric acid in the anolyte. The concentration of free phosphoric acid at the interface increases with the increase of the concentration of phosphoric acid in the bulk of the electrolyte.

* If we were to take into account the possible contribution of migration of Cu^{++} (or CuOH^+) to the mass flux, the agreement between experimental and calculated values would be further improved.

** The following assumptions are made:

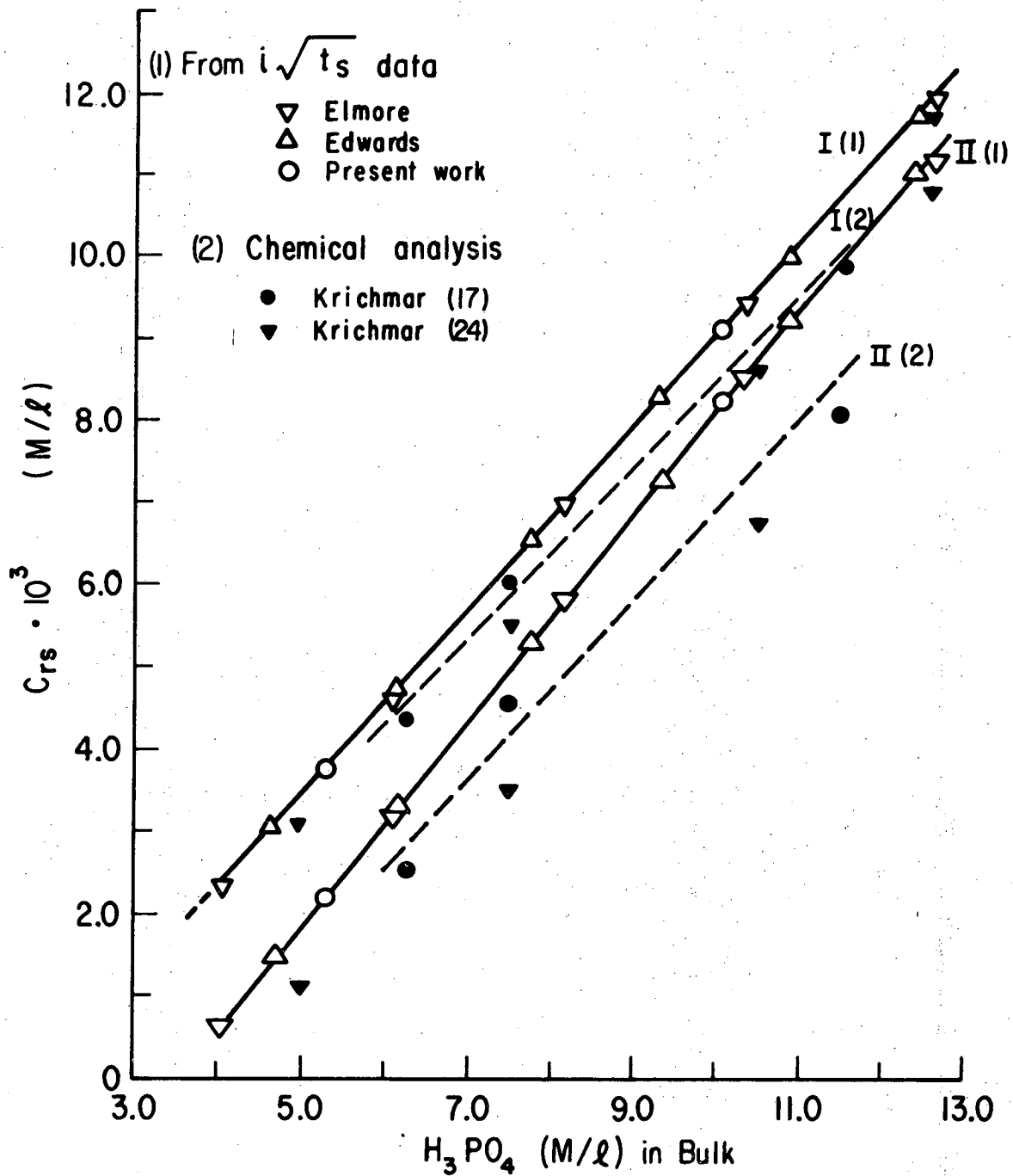
total concentration of phosphoric acid \approx free phosphoric acid concentration + concentration of phosphoric acid combined with Cu^{++}

and $\left[\begin{array}{l} \text{total concentration} \\ \text{of phosphoric acid} \end{array} \right]_{x=0} \approx \left[\begin{array}{l} \text{total concentration} \\ \text{of phosphoric acid} \end{array} \right]_{x=\infty}$



XBL 7111-7552

Fig. 9. Relation between $i\sqrt{t_s}$ calc and $i\sqrt{t_s}$ obs in the case of the reaction product control. $i\sqrt{t_s}$ calc was obtained by Eq. (12'). Range of bulk concentration of H_3PO_4 : $4 < C_{rb} < 15$ M. The slope of $i\sqrt{t_s}$ obs vs. $i\sqrt{t_s}$ calc line is about 1.1 for D_{po} and 1.3 for D'_{pm} respectively.



XBL 7111-7553A

Fig. 10. Concentration of phosphoric acid at the anode surface, C_{rs} , as the function of bulk phosphoric acid concentration, C_{rb} . Lines I(1) and I(2) are for reaction I and lines II(1) and II(2) for reaction II.

When copper phosphate deposits on the anode surface the interfacial concentration of phosphoric acid, C_{rs} , is highest for reaction I and lowest for reaction II. Simultaneous occurrence of both reactions would lead to intermediate values of C_{rs} .

The result obtained from the foregoing diffusion-kinetic study as well as the evidence for the formation of copper oxides at the current plateau (18) conclusively support the view that the first cell voltage jump in galvanostatic experiments or the current decrease in potentiostatic experiments is caused by reaching the critical solubility of copper phosphate followed by the formation of a resistive film on the anode surface.

PEAK CURRENT DENSITY

In the active dissolution of copper, the anodic current density increases with the increase of anode potential according to the Tafel relation (18). Under given hydrodynamic conditions, the concentration of copper phosphate increases with the increase of anode potential, and finally reaches the critical solubility. It is important to evaluate, whether the onset of sharp potential rise in galvanostatic (unsteady state diffusion) experiments (3,4,18) is caused by the same mass transport mechanism as the occurrence of the peak current density* phenomenon in steady state anodic polarization runs obtained in forced convection (1).

In laminar forced convection, the correlation (26,27)

$$\text{Nu} = 1.85 \left(\text{Re Sc} \frac{d}{L} \right)^{1/3} \quad (13)$$

can be used as an accurate representation of mass transfer to an electrode in a flat duct, when the concentration of a reactant or a reaction product is kept constant over the whole surface of the electrode. Nu, Re, Sc, d, and L are Nusselt number, Reynolds number, Schmidt number, equivalent duct diameter, and electrode length, respectively.

For the particular electrode configuration in a horizontal rectangular channel such as the one used by Hoar and

* Using the analysis developed by Selman (25), we find that the potential scan velocities employed by Hoar and Rothwell indeed allow reaching the steady state.

Rothwell,* the limiting current is difficult to estimate. However, the proportionality

$$\frac{i_{pk}}{F} \propto D^{2/3} V^{1/3} \Delta C \quad (14)$$

is still expected to be valid (i_{pk} is the peak current density and V is the center line velocity of flow in the duct.). For a given phosphoric acid concentration, we have $(i_{pk}/F) \propto V^{1/3}$. Examination of Hoar and Rothwell's data shows indeed proportionality of i_{pk} to $V^{1/3}$ for the entire range of H_3PO_4 concentration employed (6-10 M). This suggests that the peak current densities are greatly affected by the hydrodynamic conditions near the anode surface.

If the peak current densities are caused by the strong depletion of phosphoric acid, the values of $i_{pk}/D_r^{2/3} V^{1/3}$ should be proportional to the concentration of phosphoric acid in the bulk electrolyte, the driving force for mass transfer.

The viscosity of the electrolyte saturated with copper phosphate at the anode surface is several times higher than that of the bulk electrolyte (18,24). This should cause lowering of the diffusivity of phosphoric acid in the diffusion layer. Since there is no information

* The velocity boundary layer in this cell is not fully developed at the leading edge of the electrode. Further, because of the circular geometry of the anode, the mass transfer boundary layer thickness varies across the anode, not only in the direction of flow, but also in a direction normal (90°) to it.

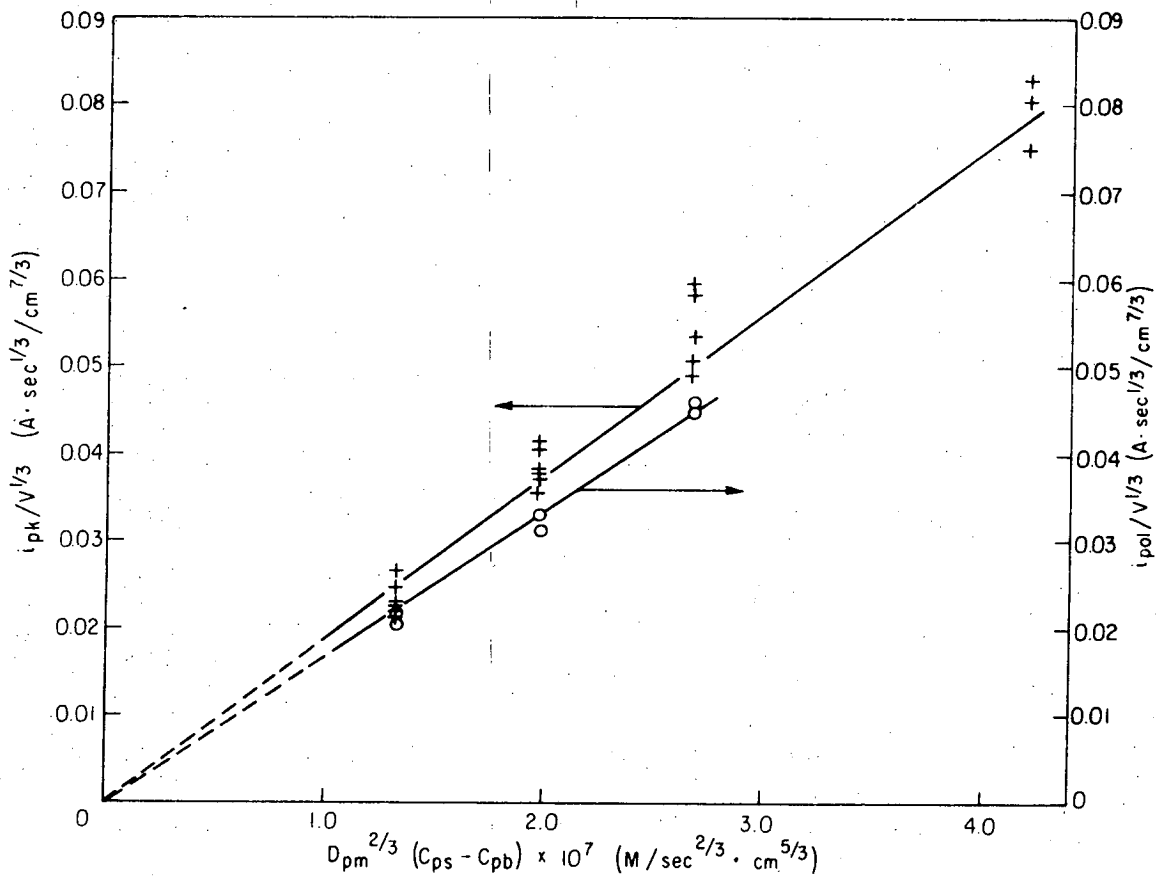
available on the effect of Cu^{++} concentration on the diffusivity of phosphoric acid, two cases are considered: a) the effective diffusivity of phosphoric acid in the diffusion layer is assumed to be equal to the diffusivity of phosphoric acid in the bulk electrolyte, D_{rb} , b) the effective diffusivity is same as the one corresponding to the concentration at the surface. Using either of these diffusivity estimates, the ratio $i_{pk}/D_r^{2/3}V^{1/3}$ decreases with increasing bulk concentration of H_3PO_4 . This result indicates that the peak current cannot be explained by the limiting transport of phosphoric acid.

If on the other hand the peak current phenomenon is caused by the attainment of the critical solubility of copper phosphate followed by the coverage of the surface by solid deposits we should expect that:

$$\frac{i_{pk}}{V^{1/3}} \propto D_{pm}^{2/3} (C_{ps} - C_{pb})^* \quad (13)$$

A reasonable confirmation of this proportionality is demonstrated in Fig. 11, in which the experimental peak current densities are those by Hoar and Rothwell (1). Again, as in the analysis of data obtained under galvanostatic conditions in pure diffusion, we conclude that the controlling step in the active dissolution range and up to the peak current is the transport of copper phosphate from the surface to the bulk electrolyte. For purposes of comparison, values of $i/V^{1/3}$ calculated with the current

* Because of a narrow range of the critical solubility of copper phosphate in the concentration range of 6 M H_3PO_4 to 10 M H_3PO_4 , proportionality of $i_{pk}/V^{1/3}$ to $D_{pm}^{2/3}(C_{ps} - C_{pb})$ is tested. $D_{pm} = (1/2)(D_{ps} + D_{pb})$.



XBL 7111-7563

Fig. 11. Relation between $i_{pk}/V^{1/3}$ or $i_{pol}/V^{1/3}$ and $D_{pm}^{2/3} (C_{ps} - C_{pb})$.
 Data from Hoar and Rothwell (1). $D_{pm} = (1/2)(D_{pb} + D_{ps})$.

density at the polishing plateau, i_{pol} , as obtained by Hoar and Rothwell, are also shown in Fig. 11. The behavior demonstrated by i_{pol} is also consistent with the controlling role of the transport of copper phosphate from the surface into the bulk electrolyte.

Concluding Remarks

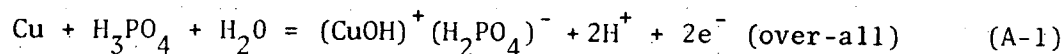
In the foregoing we have compared new results of unsteady state experiments on the anodic dissolution of copper in phosphoric acid in the active dissolution regime with those obtained earlier by Elmore and Edwards. Transition times in 5 and 10 M H_3PO_4 agree very well with those reported by the above authors. Analysis of transition times by using the best available diffusion coefficient and solubility data leads to the conclusion that in the limiting current phenomenon characteristic of the electropolishing of copper, transport of phosphoric acid is not the limiting process. The solubility limit of copper phosphate is exceeded while the concentration of phosphoric acid is still quite appreciable at the anode surface. This interpretation is congruent with the peak current density values reported by Hoar and Rothwell for electropolishing of copper in steady state laminar flow. A more precise and definitive description of the controlling transport mechanism will only be possible, when more extensive information becomes available on the properties of the ternary system $Cu^{++} - H_3PO_4 - H_2O$.

ACKNOWLEDGMENT

This work was supported by the U.S. Atomic Energy Commission.

APPENDIX Derivation of Eqs. 3-6 (see Ref. 18)

Reaction I



$$t_{\text{H}^+} + t_{\text{H}_2\text{PO}_4^-} + t_{\text{CuOH}^+} = 1 \quad (\text{A-2})$$

in which we assume only the first dissociation of H_3PO_4 and neglect $t_{\text{HPO}_4^-}$, $t_{\text{PO}_4^{3-}}$, $t_{\text{Cu}^{++}}$, and t_{OH^-} . The increase of $[(\text{CuOH})^+ (\text{H}_2\text{PO}_4)^-]$ per unit time at the anode by migration is $(i/2F)(1-t_{\text{CuOH}^+})$ and the decrease of $[\text{H}_3\text{PO}_4]$ is $(i/F)t_{\text{H}^+} - (i/2F)(1-t_{\text{CuOH}^+})$. Thus, we obtain

$$\frac{i}{2F} (1 - t_{\text{CuOH}^+}) = -D_p \nabla C_p$$

or

$$\text{for } (\text{CuOH})^+ (\text{H}_2\text{PO}_4)^- \quad (\text{A-3})$$

$$i = \frac{2F}{1-t_{\text{CuOH}^+}} D_p |\nabla C_p|$$

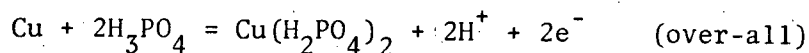
and

$$\frac{i}{F} t_{\text{H}^+} - \frac{i}{2F} (1 - t_{\text{CuOH}^+}) = D_r \nabla C_r$$

$$\text{for } \text{H}_3\text{PO}_4 \quad (\text{A-4})$$

$$i = \frac{F}{t_{\text{H}^+} - \frac{1-t_{\text{CuOH}^+}}{2}} D_r |\nabla C_r|$$

Reaction II



$$t_{\text{H}^+} + t_{\text{H}_2\text{PO}_4^-} + t_{\text{Cu}^{++}} = 1$$

The increase of $[\text{Cu}(\text{H}_2\text{PO}_4)_2]$ per unit time at the anode by migration is $(i/2F)(1-t_{\text{Cu}^{++}})$ and the decrease of $[\text{H}_3\text{PO}_4]$ is $(i/F)t_{\text{H}^+}$. Then, we obtain

$$i = \frac{2F}{1 - t_{\text{Cu}^{++}}} D_p |\nabla C_p| \quad \text{for } \text{Cu}(\text{H}_2\text{PO}_4)_2$$

and

$$i = \frac{F}{t_{\text{H}^+}} D_r |\nabla C_r| \quad \text{for } \text{H}_3\text{PO}_4$$

NOMENCLATURE

Symbol	Definition
d	Equivalent duct diameter (cm)
i	Apparent current density (A/cm^2)
i_{pol}	Current density in good electropolishing region (A/cm^2)
i_{pk}	Peak current density (A/cm^2)
n	Number of electrons transferred in the electrode process
n'	Apparent valence of a dissolved anode
t	Time (sec)
t_s	Time required for the onset of an anode potential jump (sec)
$t_{H^+}, t_{Cu^{++}}, t_{CuOH^+}$	Transference number
x	Rectangular coordinate
C(t)	Concentration at $t=t$ (mol/cm^3)
C_p	Concentration of copper phosphate (mol/cm^3)
C_{pb}	Concentration of copper phosphate in the bulk solution (mol/cm^3)
C_{ps}	Solubility of copper phosphate (mol/cm^3)
C_r	Concentration of phosphoric acid (mol/cm^3)
C_{rb}	Concentration of phosphoric acid in the bulk solution (mol/cm^3)
D	Diffusion coefficient (cm^2/sec)
D_p	Diffusion coefficient of copper phosphate (cm^2/sec)
D_{po}	Diffusion coefficient of copper phosphate at $C_p=0$ (cm^2/sec)

D_{pb}	Diffusion coefficient of copper phosphate in the bulk solution (cm^2/sec)
D_{pm}	$(1/2)(D_{ps} + D_{pb})$ (cm^2/sec)
D'_{pm}	$(1/2)(D_{ps} + D_{po})$ (cm^2/sec)
D_{ps}	Diffusion coefficient of copper phosphate at the anode surface (cm^2/sec)
D_r	Diffusion coefficient of phosphoric acid (cm^2/sec)
D_{ro}	Diffusion coefficient of phosphoric acid at $C_r \rightarrow 0$ (cm^2/sec)
D_{rb}	Diffusion coefficient of phosphoric acid in the bulk solution (cm^2/sec)
D_{rs}	Diffusion coefficient of phosphoric acid at the anode surface (cm^2/sec)
D_{rm}	$(1/2)(D_{rb} + D_{rs})$ (cm^2/sec)
D'_{rm}	$(1/2)(D_{rb} + D_{ro})$ (cm^2/sec)
F	Faraday's constant (96500 coul/gm.eq.)
I	Total current (A)
L	Electrode length (cm)
M	Molecular weight of a dissolved metal (g/mol)
V	Center line velocity of flow in a rectangular channel (cm/sec)
ΔW	Weight loss of an anode specimen (g)

Dimensionless numbers

Nu	Nusselt number
Re	Reynolds number
Sc	Schmidt number

References

1. T. P. Hoar and G. P. Rothwell, *Electrochimica Acta* 9, 135 (1964).
2. Z. Zembura, *Bull. Acad. Polon. Sci. Cl. XI*, No. 5, 271 (1963).
3. J. Edwards, *J. Electrochem. Soc.* 100, 223C (1953).
4. W. C. Elmore, *J. Appl. Phys.* 11, 797 (1940).
5. S. I. Krichmar, *Proc. Acad. Sci. U.S.S.R., Sect. Phys. Chem.* 114, 303 (1957).
6. G. S. Vozdvizhensky and A. I. Turashev, *Dokl. Akad. Nauk. SSSR*, 114, 358 (1957).
7. A. Hickling and J. K. Higgins, *Trans. Inst. Metal Finishing* 29, 274 (1953).
8. M. C. Petit, *Electrochimica Acta* 8, 217 (1963).
9. C. Wagner, *J. Electrochem. Soc.* 101, 225 (1954).
10. W. C. Elmore, *J. Appl. Phys.* 10, 724 (1939).
11. K. F. Lorking, *Electrochimica Acta* 7, 101 (1962).
12. K. Ohashi, T. Murakawa, and S. Nagaura, *J. Electrochem. Soc. Japan* 30, 165 (1962).
13. M. Novak, A. K. Reddy, and H. Wroblowa, *J. Electrochem. Soc.* 117, No. 6, 733 (1970).
14. H. S. Carslaw and J. C. Jaeger, *Conduction of Heat in Solids*, 2nd Ed., Oxford (1959).
15. Marie-Claude Petit and M. Roger Schmitt, *Compt. rend.* 254, 2569 (1962).
16. D. Laforgue-Kantzer, *Compt. rend.* 233, 547 (1951).
17. S. I. Krichmar and V. P. Galushko, *Russ. J. Inorganic Chem.* 1, No. 10, 2422 (1956).

18. K. Kojima, Ph.D. Thesis, Univ. of California, Berkeley (1972).
19. O. W. Edwards and E. O. Huffman, J. Phys. Chem. 63, 1830 (1959).
20. S. I. Krichmar, A. Ya. Pronskaya, and K. F. Afendik, Soviet Electrochem. 2, No. 8, 896 (1966).
21. M. Kerker and W. F. Espenscheid, J.A.C.S. 80, 776 (1958).
22. T. W. Chapman, Ph.D. Thesis, Univ. of California, Berkeley (1967).
23. K. Kojima and C. W. Tobias, IMRD Annual Report, UCRL-18735, p. 35 (1968).
24. S. I. Krichmar, Russ. J. Phys. Chem. 39, No. 4, 433 (1965).
25. J. R. Selman, Ph.D. Thesis, Univ. of California, Berkeley (1971).
26. R. H. Norris and D. D. Streid, Trans. A.S.M.E. 62, 525 (1940).
27. R. G. Hickman, Ph.D. Thesis, Univ. of California, Berkeley (1963).
28. K. Kinoshita, private communication.

LEGAL NOTICE

This report was prepared as an account of work sponsored by the United States Government. Neither the United States nor the United States Atomic Energy Commission, nor any of their employees, nor any of their contractors, subcontractors, or their employees, makes any warranty, express or implied, or assumes any legal liability or responsibility for the accuracy, completeness or usefulness of any information, apparatus, product or process disclosed, or represents that its use would not infringe privately owned rights.

TECHNICAL INFORMATION DIVISION
LAWRENCE BERKELEY LABORATORY
UNIVERSITY OF CALIFORNIA
BERKELEY, CALIFORNIA 94720